Ultra-thin Graphene Metasurface as Tunable Absorber and Terahertz Refractive Index Sensor

Naveen Kumar Maurya*(1) and Anil Kumar Nayak(2)
(1) Department of ECE, Vishnu Institute of Technology, Bhimavaram-534202, Andhra Pradesh, India
(2) Department of ECE, Indian Institute of Technology Indore, Indore-453552, Madhya Pradesh, India
Corresponding Author*: naveenkumar.m@vishnu.edu.in

Abstract

This paper presents an ultra-thin multifunctional metasurface capable of working as both a tunable absorber and refractive index (RI) sensor in the terahertz (THz) regime. Considering an absorber application, metasurface covers a very wide tuning range from 2.38 to 5.25 THz with absorptivity $(A(f)) \geq 90\%$. In contrast, when working as a RI sensor, metasurface provides a sensitivity (S) and quality factor (Q) of 0.8 THz/RIU and 5.95, respectively. The working principle is based on the generation of the plasmonic mode at the graphene-dielectric interface by intelligently exciting one-wavelength loop mode without disturbing the symmetricity in the top graphene pattern.

1 Introduction

The efficacy of metasurfaces to control and manipulate the propagation of electromagnetic (EM) waves has made them a crucial device for numerous applications in the terahertz (THz) regime [1, 2]. With the advent of new wireless technologies, the need for smart THz metasurfaces with tunable frequency characteristics has also gone up. Interestingly, the discovery of monolayer graphene has made metasurface frequency tunable with a simpler biasing technique, unlike the complex biasing mechanism of varactor and pin diodes [3–6]. Since THz systems are quite compact, the need for size-constrained metasurfaces that can perform more than one task is increasing significantly [7, 8]. All these technological advancements and challenges have inspired researchers to design and develop graphene-based tunable and multifunctional metasurfaces.

To date, many graphene-based tunable metasurface absorbers (TMSAs) have been reported [9–11]. [9] has used a square graphene ring to design TMSA, whereas a combination of circular rings with a cross strip made up of graphene has been used in [10] to attain tunability. A unique combination of elliptical graphene strips connected in a closed loop is introduced in [11]. All these graphene TMSA are restricted to the absorber application only. In contrast, metasurfaces are also employed for sensing application [12, 13]. The work reported in [12] has used rectangle-shaped meta-atom made up of gold, whereas [13] has used fractal resonators designed using aluminum. Here also these absorbers are restricted to only sensing applications and cannot be employed for tunable absorber applications.

Eventually, the graphene perfect absorber reported in [14] could be used as both a tunable absorber and refractive index (RI) sensor. So far, very less works have been reported on multifunctional metasurface absorbers. Hence, there is a need of an hour to design MSAs that can perform more than one task. This work presents a graphene-based TMSA, which can provide a very wide tuning range from 2.38 to 5.25 THz with absorptivity $(A(f)) \geq 90\%$ when working as an absorber. Whereas, metasurface provides a sensitivity (S) and quality factor (Q) of 0.8 THz/RIU and 5.95, respectively, when it works as a RI sensor.

2 Metasurface for Absorber Application

The schematic view of the proposed TMSA designed using graphene on the silicon dioxide (SiO_2) substrate has been depicted in Fig. 1. The metasurface response when it interact with incident plane wave has been shown in Fig. 2. Since the transmission coefficient ($|S_{21}|$) is almost negibible, the absorptivity $(A(f))$ has been calculated using Eq. 1 and the absorption mechanism depend upon the impedance matching between TMSA and free space [15]. The TMSA provides near-unity $A(f)$ at 2.38 THz with a

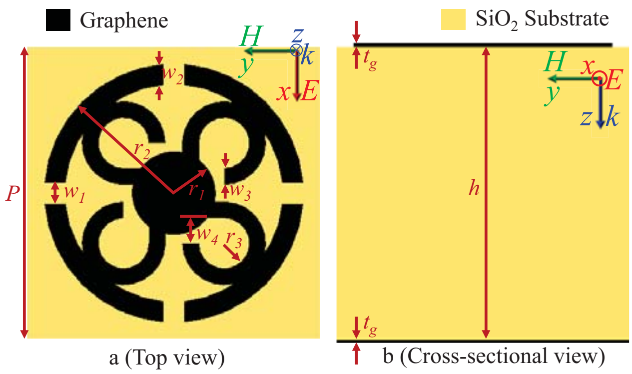

Figure 1. Schematic diagram of TMSA: (a) top and (b) cross-sectional view. $P = h = 7$, $r_1 = 1$, $r_2 = 3.1$, $r_3 = w_4 = 0.6$, $w_1 = w_2 = 0.5$, $w_3 = 0.4$ (unit:μm), $t_g = 0.335$ nm, $\mu_c = 0.2$ eV, $\tau = 1$ ps, $T = 300$ K.

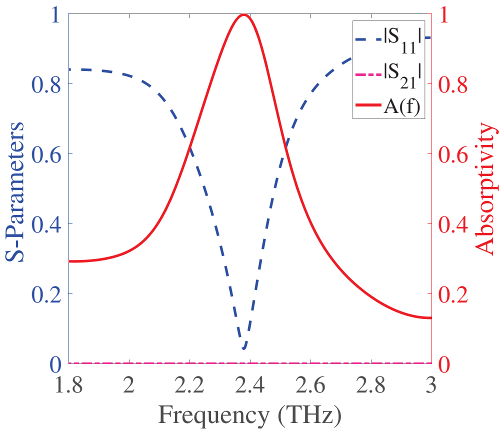

Figure 2. $|S_{11}|$, $|S_{21}|$ and $A(f)$ of TMSA.

bandwidth (BW) of 0.14 THz for $A(f) \geq 90\%$. The periodicity and thickness of TMSA are $\lambda_0/18$, where λ_0 is computed at 2.38 THz. The compactness design and ultra-thin profile makes TMSA suitable for EM shielding.

$$A(f) = 1 - |S_{11}|^2 \qquad (1)$$

,where $|S_{11}|$ is the reflection coefficient.

The working principle of the TMSA is quite simple, which is based on the generation of the plasmonic mode/surface plasmon polaritons (SPPs) at the graphene-dielectric interface by intelligently exciting one-wavelength loop mode without disturbing the symmetricity in the top graphene

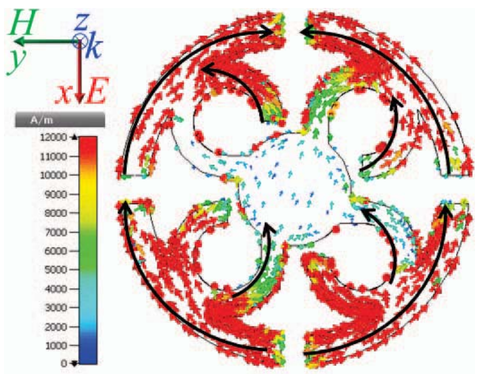

a

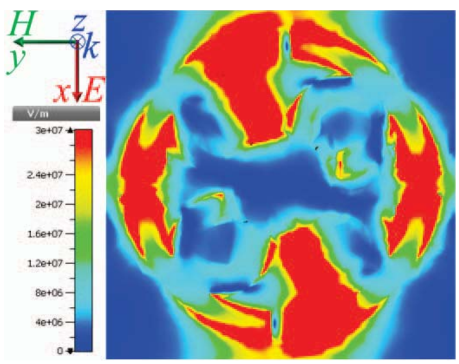

b

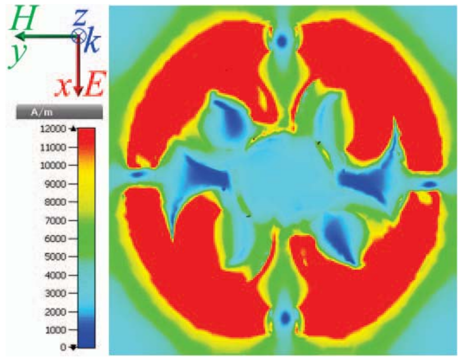

c

Figure 3. Modal distribution at 2.38 THz in xy-plane: (a) J_{surf}, (b) electric, and (c) magnetic.

pattern as shown in Fig. 3. The surface current distribution (J_{surf}) on the top graphene pattern shows the excitation of one-wavelength loop mode in the outer splitted circular ring resonator as shown in Fig. 3a. The splits are introduced to create the E-field coupling for the strong localization of SPP waves in the gap as shown in Fig. 3b. In addition, four circular arc-shaped resonators connected with a central graphene disk have been used to excite the same J_{surf} to that of one-wavelength loop mode in the outer circular ring resonator by nullifying the effect of splits on the modal distribution as shown in Fig. 3a. The TMSA also responds well to the H-field vector of incident EM wave as shown in Fig. 3c. Hence, the proposed design shows a strong response to both the E-field and H-field components of the incident plane wave and is found to be better in terms of excitation of SPP mode in the graphene ring compared with a simple circular ring resonator.

The angular stability in the $A(f)$ for different polarization (ϕ) and incidence angle (θ) under transverse magnetic (TM) polarization has been shown in Fig. 4a and b, respectively. The TMSA is insensitive to the ϕ and provides $A(f) \geq 90\%$ up to $\theta \leq 60°$. Similar behavior has been found for transverse electric polarization, which is not shown here due to brevity.

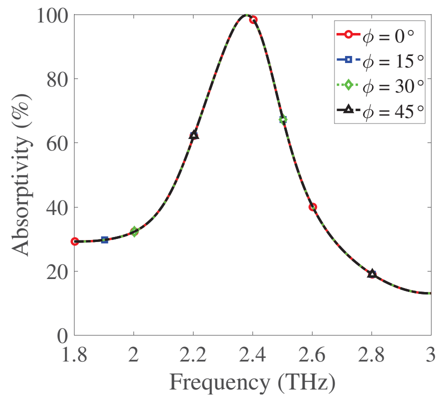

a

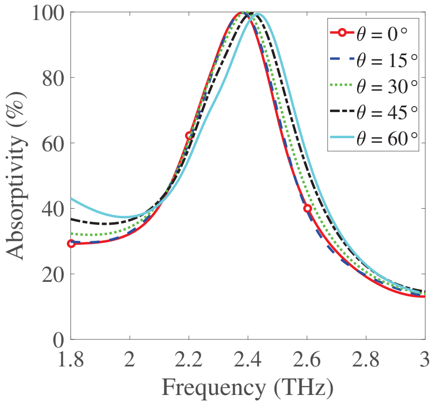

b

Figure 4. $A(f)$ for different: (a) ϕ and (b) θ (TM).

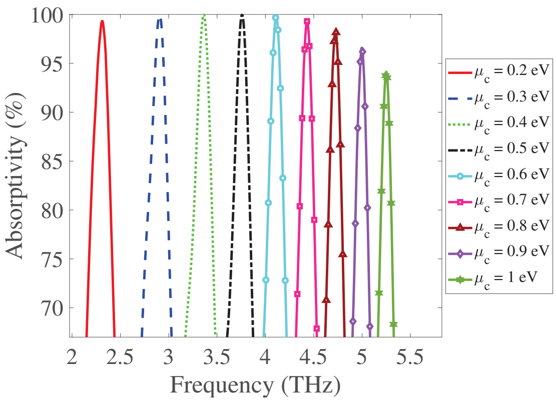

Figure 5. $A(f)$ for different μ_c

As discussed in the introduction, tunable $A(f)$ reponse is the need of an hour for the smart THz applications. In this context, the chemical potential (μ_c) has been varied keep all other electrical and physical parameters unchanged as shown in Fig. 5. It is evident that with an increse in μ_c from 0.2 to 1 eV the peak of the absorption curve moves from 2.38 to 5.25 THz, thus providing a tuning range of 2.87 THz. The TMSA shows an excellent right shift in absorption response with the increase in μ_c. The tunability has been achieved by varying surface conductivity of the graphene, which is the function of μ_c [16–18].

3 Metasurface for Refractive Index (n) Sensing Application

The TMSA discussed in section 2 could be directly used for RI sensing by loading analyte under test (AUT) on the top surface of TMSA as shown in Fig. 6a. The AUT may be any body fluid such as blood, urine, etc. It is worth mentioning here that the blood or urine of a patient with no medical condition could be mapped by its corresponding value of refractive indices (n) and resonance frequency (f_r), which differs for the case where the patient has any medical issues. Hence, the variation in the value of 'n' could be used for the diagnosis of diseases often called biosensing [19]. Fig. 6b shows that with the increase in 'n' of the AUT, the peak of the absorption curve moves towards the lower frequency spectrum, thus pointing to a distinct f_r. The mapping between 'n' and f_r shows almost linear variation as shown in Fig. 6c. RI sensor provides a sensitivity (S) and quality factor (Q) of 0.8 THz/RIU and 5.95, respectively. Hence, the proposed TMSA could be used for biosensing applications in the THz regime.

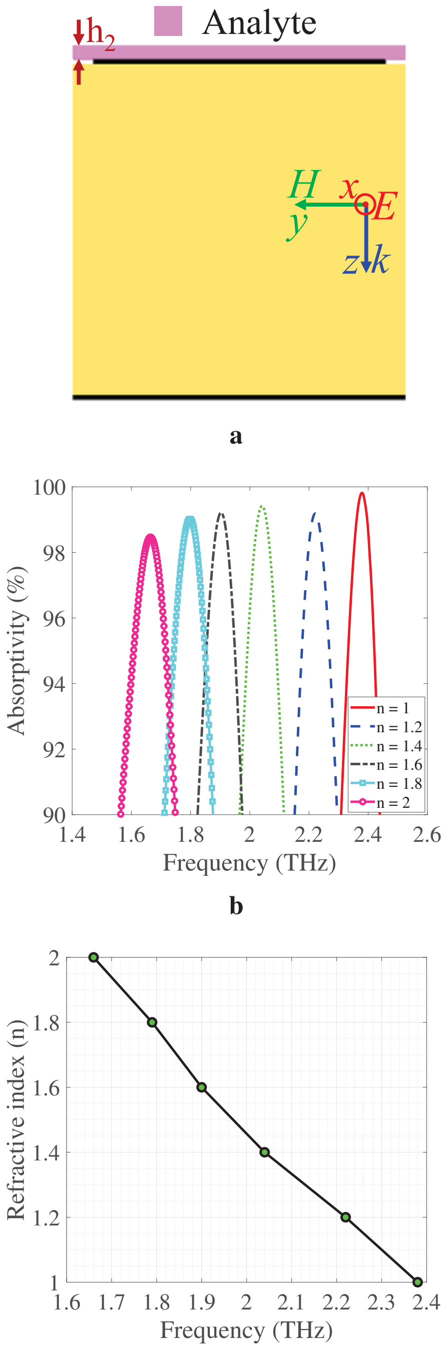

c

Figure 6. (a) RI sensor in yz-plane with analyte under test $h_2 = 0.4$ μm, (b) $A(f)$ for different n and (c) n vs f_r.

4 Conclusion

This paper presents a multifunctional TMSA. The simplicity of the unit cell geometry and physics-based design approach shows the efficacy of the proposed work. Future work could focus on implementing multi-band TMSA for more reliable sensing.

5 Acknowledgements

Thanks to Dr. Anil Kumar Nayak for the simulation of the work using CST Studio Suite during his PhD tenure at the Indian Institute of Technology Roorkee.

References

[1] J. He, T. Dong, B. Chi, and Y. Zhang, "Metasurfaces for terahertz wavefront modulation: a review," *Journal of Infrared, Millimeter, and Terahertz Waves*, vol. 41, no. 6, pp. 607–631, 2020.

[2] N. K. Maurya, J. Ghosh, and P. Sumithra, "Design of graphene-based tunable ultra-thin uwb metasurface for terahertz regime," *Optik*, vol. 279, p. 170753, 2023.

[3] A. C. Neto, F. Guinea, N. M. Peres, K. S. Novoselov, and A. K. Geim, "The electronic properties of graphene," *Reviews of modern physics*, vol. 81, no. 1, p. 109, 2009.

[4] N. K. Maurya, S. Kumari, P. Pareek, and G. Varshney, "Highly-efficient tunable dipole-driven yagi–uda antenna with end-fire radiation for terahertz application," *Nano Communication Networks*, vol. 38, p. 100480, 2023.

[5] C. Ram, M. Kartikeyan, and S. Yuvaraj, "Spoof surface plasmons based reconfigurable bandstop filter for thz applications," *Optical and Quantum Electronics*, vol. 56, no. 1, p. 27, 2024.

[6] N. K. Maurya, S. Kumari, P. Pareek, and L. Singh, "Graphene-based frequency agile isolation enhancement mechanism for mimo antenna in terahertz regime," *Nano Communication Networks*, vol. 35, p. 100436, 2023.

[7] J. Wang, R. Yang, R. Ma, J. Tian, and W. Zhang, "Reconfigurable multifunctional metasurface for broadband polarization conversion and perfect absorption," *IEEE Access*, vol. 8, pp. 105 815–105 823, 2020.

[8] H. L. Wang, H. F. Ma, M. Chen, S. Sun, and T. J. Cui, "A reconfigurable multifunctional metasurface for full-space control of electromagnetic waves," *Advanced Functional Materials*, vol. 31, no. 25, p. 2100275, 2021.

[9] K. V. Babu, P. Das, S. Das, A. H. Almawgani, T. Islam, and A. R. Alhawari, "Design of graphene-based broadband metamaterial absorber with circuit analysis approach for terahertz region applications," *Optical and Quantum Electronics*, vol. 55, no. 13, p. 1188, 2023.

[10] A. Verma and O. P. Meena, "Dual-band polarization insensitive graphene-based reconfigurable absorber in a terahertz regime," *Applied Optics*, vol. 63, no. 8, pp. 1934–1938, 2024.

[11] Q. Zhou, P. Liu, L.-a. Bian, X. Cai, and H. Liu, "Multi-band terahertz absorber exploiting graphene metamaterial," *Optical Materials Express*, vol. 8, no. 9, pp. 2928–2940, 2018.

[12] R. Agrahari, S. Dwivedi, P. K. Jain, and M. Mahto, "High sensitive metasurface absorber for refractive index sensing," *IEEE Transactions on Nanotechnology*, 2023.

[13] Y. I. Abdulkarim, O. Altintas, A. S. Karim, H. N. Awl, F. F. Muhammadsharif, F. O. Alkurt, M. Bakir, B. Appasani, M. Karaaslan, and J. Dong, "Highly sensitive dual-band terahertz metamaterial absorber for biomedical applications: simulation and experiment," *ACS omega*, vol. 7, no. 42, pp. 38 094–38 104, 2022.

[14] P. Wu, X. Zeng, N. Su, M. Chen, Y. Zeng, and Y. Yu, "A graphene perfect absorber with tunable, dual band, high sensitivity characteristics," *Diamond and Related Materials*, vol. 125, p. 109002, 2022.

[15] N. K. Maurya, J. Ghosh, S. Subramanian, P. Pareek, L. Singh, and K. Srinivas, "Tunable ultra-wideband graphene metasurface absorber: A mode merger design approach for terahertz applications," *Optics Communications*, vol. 550, p. 129991, 2024.

[16] C. S. Kaipa, A. B. Yakovlev, G. W. Hanson, Y. R. Padooru, F. Medina, and F. Mesa, "Enhanced transmission with a graphene-dielectric microstructure at low-terahertz frequencies," *Physical Review B*, vol. 85, no. 24, p. 245407, 2012.

[17] G. W. Hanson, "Dyadic Green's functions and guided surface waves for a surface conductivity model of graphene," *Journal of Applied Physics*, vol. 103, no. 6, p. 064302, 2008.

[18] N. K. Maurya and J. Ghosh, "Ultrathin tunable uwb metasurface absorber design by exciting plasmonic modes in bilayer graphene stack," *Diamond and Related Materials*, vol. 145, p. 111065, 2024.

[19] S. Seyyedmasoumian, A. Attariabad, A. Pourziad, and M. Bemani, "Refractive index biosensor using metamaterial perfect absorber based on graphene in near-infrared for disease diagnosis," *IEEE Sensors Journal*, vol. 22, no. 15, pp. 14 870–14 877, 2022.